Nano-positioning using an adaptive pulse width approach

S Zelenika[1,2*] and **F De Bona**[2]
[1]University of Rijeka, Faculty of Engineering, Rijeka, Croatia
[2]Dipartimento di Ingegneria Elettrica Gestionale e Meccanica, Università di Udine, Udine, Italy

The manuscript was received on 19 December 2008 and was accepted after revision for publication on 14 January 2009.

DOI: 10.1243/09544062JMES1489

Abstract: Macro- and micro-dynamic mechanical non-linearities limiting the precision of conventional DC motor-driven positioning systems based on sliding and rolling elements have been characterized experimentally via a laser interferometric system. The obtained results confirm recent tribological models. In particular, the parameters describing the non-linear elastic and plastic phenomena related to pre-sliding displacement have been identified and used to develop an integrated system model. It was therefore possible to prove that, in the range of displacements corresponding to the pre-sliding phase, there is a quadratic dependence between the duration of an actuating impulsive force and the resulting displacement. According to a pulse width scheme, a control law has been implemented whose adaptive structure compensates for the position and time variability of the observed non-linear effects. The application of the proposed approach to both short and long travel ranges and the reached nanometric accuracies confirm the applicability of the proposed control scheme to compensate concurrently the macro- and the micro-dynamic effects.

Keywords: nano-positioning, mechanical non-linearities, pre-sliding displacement, pulse width actuation

1 INTRODUCTION

In the design of high-precision positioning systems, a solution based on sliding and rolling devices is frequently adopted. The usage of such mechanical systems limits, however, positioning precision in modern machine tools, optical systems, robots, scientific instrumentation, semiconductor technology, measurement equipment, etc. [**1**, **2**]. It is well known that in this case precision is significantly influenced by the presence of two types of mechanical non-linearities, which are usually referred to as 'macro-dynamic' phenomena (stiction, Coulomb friction, viscous friction, backlash) and 'micro-dynamic' phenomena (pre-sliding displacements, i.e. displacements that occur even for loads smaller than those needed to overcome stiction [**3**–**8**]).

Corresponding author: Department of Mechanical Engineering Design, University of Rijeka, 58 Vukovarska, Rijeka 51000, Croatia. email: sasa.zelenika@riteh.hr

It has been extensively demonstrated that the compensation of these mechanical non-linearities has to be based on properly designed servo control typologies [**3**, **9**–**11**]. The requirement to achieve high precision is nowadays generally met by applying dual-mode control, where one controller is used to compensate the macro-dynamic phenomena, while another control typology is used for the micro-dynamic non-linearities. Switching between the two controllers is performed in the micrometric region, i.e. coarse actuation is used to bring the system in the vicinity of the reference position where fine actuation is used.

In reference [**12**] the macro-dynamics of a lead screw-based positioning system is modelled by a system equilibrium equation including a constant Coulomb friction force and a viscous friction coefficient. On the other hand, the micro-dynamics of the system is dealt with by adding into the system a non-linear function with a rule-based PID tuning method. This non-model-based approach allows high positioning speed to be obtained, but with micrometric accuracy only. Moreover, the adopted control strategy

is limited by the fact that the characteristics obtained from off-line experiments do not take into account the position and time dependence of friction.

In reference [**4**] a model-based approach for the positioning of a ball-screw-driven stage is proposed. The macro-level model of friction is more accurate and based on the well-known bristle scheme developed in reference [**13**] (known also as the LuGre model [**14, 15**]), where the deformation of elastic bristles between bodies in relative motion gives rise to frictional forces. The pre-sliding (i.e. static friction) regime is described by a simplified linearized version of the model developed in reference [**16**]. Off-line system identification is necessary in this case as well. Moreover, the control design technique requires the bounds of external disturbances to be known in advance.

In reference [**17**], a similar approach is proposed: a simplified version of the micro-dynamics model given by Futami *et al.* [**6**] is used. A dual control law guaranteeing a smooth transition into the micro-dynamics region is implemented permitting a positioning error of 10 nm for linear motor-driven guides to be achieved. The approach requires an off-line identification of system parameters. In general, its applicability in the case of position variability of system parameters is not assured, as an experimental investigation of the uncertainties of the disturbance bounds is required.

In reference [**8**], the macro- and micro-dynamic regions of a ball-screw-driven stage are described by using again the friction model proposed in reference [**13**] and the pre-sliding model of reference [**16**]. An adaptive sliding mode controller is used to obtain nanometric accuracy. The method requires a preliminary experimental evaluation of all the parameters of both models. This could, however, require a tedious trial and error approach [**16**].

Recent literature confirms, thus, a tendency towards using dual-mode control laws where the models used to describe the macro- and micro-dynamic friction regimes are usually different and quite complex, often requiring an experimental evaluation of system parameters. It would seem, however, that, regardless of the used control laws, obtained accuracies are limited only by those of the measurement systems used as position sensors in the feedback loop.

The aim of this work is to develop a simple control approach, where a unique control law is applied both in the macro- and in the micro-dynamic regions. The possibility of using an adaptive control approach developed by Yang and Tomizuka [**18**], well established when macro-dynamic phenomena are to be overcome, will thus be explored with the purpose of extending its applicability to the micro-dynamics region.

The adopted models for the macro-dynamic and the micro-dynamic friction phenomena will thus be described in the following section. The respective system parameters will be identified on an experimental set-up. The adopted control typology based on an adaptive pulse width scheme will be given in section 3, where a mathematical model encompassing all the non-linear effects will be described. The identification of the relation between pulse width and the resulting displacement will allow then to apply in section 4 the developed approach to high precision positioning on short (10 μm) and relatively long (1 mm) travel ranges. In all the considered cases, nanometric accuracies are achieved, since the proposed system compensates concurrently the macro- as well as micro-dynamic non-linearities. A physical interpretation of the observed behaviour is finally given.

2 SYSTEM DESCRIPTION

2.1 Experimental set-up

Figure 1 shows the scheme of the system developed for the experimental study. It consists of a DC motor and a gear reducer, connected by means of an elastic joint to a lead screw-nut drive mechanism that converts motor rotation into the translation of a guide with free rolling elements (balls). A spring with a slight pre-load is used to compensate for backlash. It must be pointed out that standard mechanical components without particular accuracy requirements have been employed.

The position feedback signal is obtained by using a Michelson-type laser-Doppler interferometer system for non-contact measurements, permitting a resolution of 10 nm to be obtained. The uncertainty in the stage linear displacement measurements was evaluated according to the procedure suggested by Steinmetz [**19**]. In the case of a maximum stage travel of $X_{sl} = 10$ mm, an interval of uncertainty of ±20 nm was obtained. The use of an interface board provides an analogue signal (maximum range ±10 V) that is proportional to actual displacement. This signal is then read by the control unit, a floating-point digital signal processor (DSP – model TMS320C31 by Texas Instruments). This board is used to control the motor and allows the implementation of linear and non-linear control typologies by using algorithms written in C

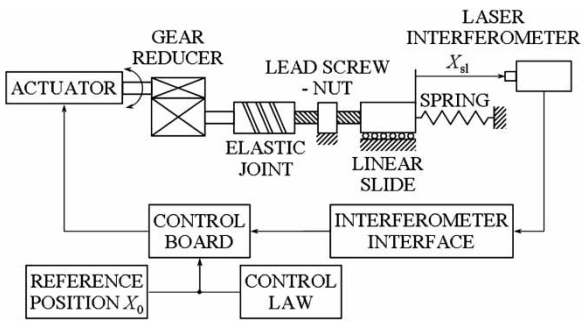

Fig. 1 Scheme of the experimental set-up

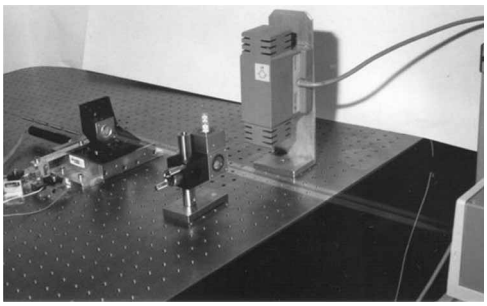

Fig. 2 Set-up of the measurement system (clearly visible are actuator, linear slide, interferometer, and laser head)

with libraries including predefined control functions. The actual set-up of the system is shown in Fig. 2.

2.2 Macro-dynamics mechanical non-linearities

The most important macro-dynamics mechanical non-linearities are represented by static, Coulomb, and viscous friction [**3**, **18**]. In order to establish the dependence of frictional loads on system motion, a simple measurement procedure [**20**] was followed. It can, in fact, be shown that angular velocity is proportional to the voltage applied to the motor, while the absorbed current is proportional to frictional torque. Therefore, the mechanical non-linearities of the system referred to the motor axis can be identified via a measurement of electrical parameters. To evaluate the contribution of all the elements of the electromechanical positioning system, the procedure was first applied to the motor alone, and then it was repeated by adding in the other elements of the kinematics chain one by one. In all the cases the measurement was repeated in 10 different positions. By comparing the frictional loads of the single elements of the positioning system, it was established that the main contribution is that of the DC motor. In fact, when the contributions of the downstream elements are referred to the motor axis, the corresponding frictional torques must be reduced proportionally to the speed ratios.

Figure 3 shows the dependence of frictional torque M_f on angular velocity ω for the whole system. The characteristic Stribeck curve can be clearly observed, where the viscous component is mainly caused by the back-electromagnetic force of the motor. This type of behaviour is typical of positioning systems driven by DC motors and it is in perfect agreement with recent tribological models [**3**, **21**–**23**]. Figure 3 shows also the frictional torque interval of uncertainty resulting from repeated measurements; the considerable dispersion (up to ±15 per cent) is mainly caused by the variability of friction. In fact, it has been extensively proven that friction phenomena have a significant dispersion due to microwear, position dependency,

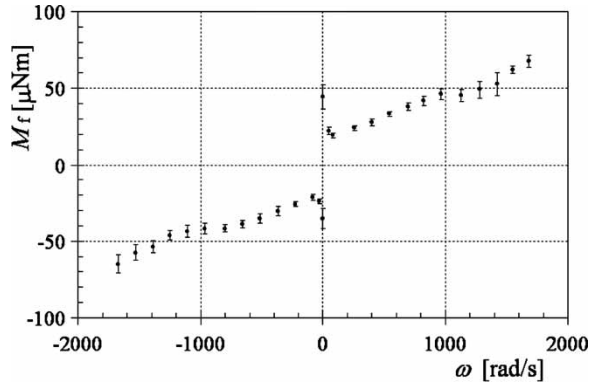

Fig. 3 Friction and its dispersion

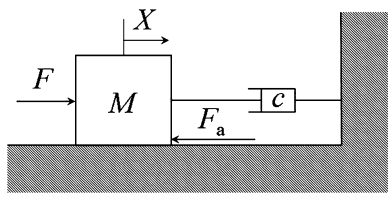

Fig. 4 Macro-dynamics model

as well as time variability of temperature and lubrication conditions. Secondary effects such as frictional memory and rising static friction (influence of the history of motion on the value of the frictional force) can then enhance these effects [**3**, **24**]. Similar percentage values of frictional dispersion were reported also by Yang and Tomizuka [**18**], where the case of accurate positioning systems involving only macro-dynamics effects was considered.

The experimental set-up of this work can be modelled physically by the equivalent translational mass–damper–friction system shown in Fig. 4. From the measurements of Fig. 3 it is hence possible determining the model parameters referred to the translation axis as: mass $M = 0.723$ Gg, static friction $F_s = 274$ N, Coulomb friction $F_c = 152$ N, and viscous damping coefficient $c = 967\,167$ kg/s.

2.3 Micro-dynamics mechanical non-linearities

In the case of positioning systems that should achieve nanometric accuracy, the micro-dynamics behaviour has to be considered. As already pointed out, this behaviour is sometimes termed also static friction, pre-sliding phenomenon, or stiction. It is basically constituted by the non-linear motion induced by forces smaller than those necessary to overcome the static friction force. Physically, at the microscopic level, friction is, in fact, due to linkages between asperities on contact surfaces. Pre-sliding motion occurs when shear stresses deform elasto-plastically the asperities [**5**]. Recently an elaborated phenomenological dynamics model in the pre-sliding region was

developed [**16**] and applied to nanometric positioning [**4, 8, 25**]. The model includes a non-linear elastic spring serially connected to a plastic module, the latter experimentally observed but not included in any of the previous pre-sliding models (see, for example, reference [**13**]. Other authors model the phenomenon even as piecewise linear [**6**]). A viscous damper characterized by a coefficient c_s, which takes into account the energy dissipation of the phenomenon, is also included (Fig. 5). The non-linear elastic module models the hysteresis by using three scalar parameters indicated, respectively, with k_1, k_2, and β. The plastic module, characterized by creep and work hardening, has as system parameters α, λ, and n.

According to the somewhat cumbersome and generally rather qualitative trial-and-error procedure described in reference [**16**], parameters n and λ, related to work hardening, are determined from a static test. In the case of the positioning system considered in this work, the test was performed by gradually loading the linear slide mounted on an optical bench. In fact, considering the speed ratios of the elements of the experimental set-up, displacement accuracies in the nanometric range imply that the linear slide will certainly be in the pre-sliding regime. An increment of loading was performed only when the system came to an almost complete rest since nanometric level motion is observed even after extended periods of time. The resulting displacement X_{sl} of the stage was measured making use of the Michelson-type laser-Doppler interferometer system (see Fig. 6). The measurements were performed up to the point at which stiction breakaway occurred, i.e. in the region where $X_{sl} = x$. The load-displacement characteristic was also recorded when unloading the system starting from different load levels.

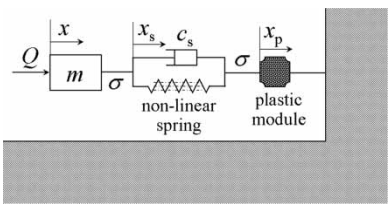

Fig. 5 Micro-dynamics model

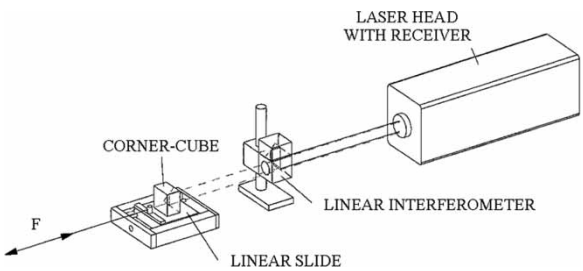

Fig. 6 Measurement of pre-sliding displacement

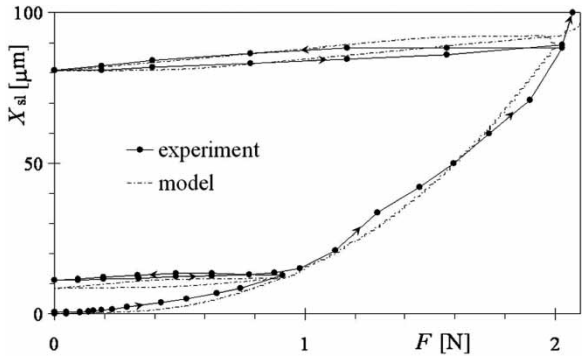

Fig. 7 Pre-sliding displacement vs. applied force

In Fig. 7 the load-displacement characteristic obtained by averaging 10 measurements is shown. In the whole measuring range a maximum interval of uncertainty (not shown in the figure for clarity reasons) of ±6 per cent was assessed, confirming that, as already noticed by Courtney-Pratt and Eisner [**5**], micro-dynamic phenomena have a relevant stochastic component. It can be observed that, before the load reaches stiction breakaway, a significant displacement is obtained. The measured displacement is a non-linear function of the applied load. When the system is unloaded, it travels back, but the resulting displacement is significantly smaller than the displacement obtained in the loading phase. Moreover, the displacement versus load characteristic during unloading is almost linear, with a mean slope that remains almost constant independently of the load at which unloading is started.

In accordance with reference [**16**], the determined parameters are then, respectively, $n = 2.81$ and $\lambda = 0.09$. The curve of Fig. 7 allows also the non-linear elastic module parameters k_1 (corresponding to the stiffness of the equivalent non-linear spring at the end of the hysteresis loop), k_2 (stiffness $(k_1 + k_2)$ corresponds to that of the equivalent non-linear spring at the reverse point of the hysteresis loop), and β (with k_2 related to the force-to-displacement characteristic of the hysteresis loop) to be assessed. According to the procedure given in reference [**16**], for the considered experimental set-up these parameters are then, respectively, $k_1 = 0.13$ N/m, $k_2 = 2.13$ N/m, and $\beta = 5$.

Parameters α and c_s are determined from dynamic tests described in reference [**16**]. Parameter α, related to creep, is determined from step force inputs, and in this case its value is $\alpha = 1$. Finally, ramping the input force to the linear stage and then suddenly removing it, allows the damping ratio and consequently the damping coefficient to be determined as $c_s = 0.9$ kg/s.

In reference [**16**] and other literature, as well as from the experimental results given in Fig. 7, it is clearly shown that the micro-dynamics phenomenon has a marked variability due again to position and time variance of friction. The dotted line of Fig. 7, representing

the results obtained by using the Hsieh model [**16**] with the above values of the characteristic parameters, matches, however, excellently the results obtained experimentally performing the described static tests on the linear slide.

3 ADAPTIVE PULSE WIDTH APPROACH

As pointed out previously, the presence of non-linearities caused by friction and their time and position variability implies the necessity of adopting a suitable control law. It has been extensively shown that friction gives rise to steady-state errors and limit cycles [**13, 18**]; as confirmed by the results shown in Fig. 3, friction variability can also affect significantly positioning precision.

There is a broad literature describing various control typologies that allow compensating these effects [**3, 15**]. In the case when simple positioning (as opposed to trajectory tracking) is sought, the adaptive control typologies based on pulse width modulation (PWM) constitute certainly one of the most efficient solutions [**3**]. In fact, as everyday experience shows, when small corrective movements are needed to reach the desired position, the application of impulsive loads permits static friction to be overcome without an excessive overshoot caused by the rapid reduction of resistive loads at stiction breakaway.

3.1 Compensation of macro-dynamics non-linearities

In this work the PWM procedure proposed by Yang and Tomizuka [**18**], applied to the equilibrium of the equivalent mechanical model of Fig. 4, will be used. According to the classical friction model, the friction force F_a will assume the value F_s, F_c or it will vanish depending on the velocity of motion of mass M. The control law described in reference [**18**] is derived from a model-based adaptive friction compensation via the control of the time duration (width) of the actuating impulse $F(t) = F_{imp}(t)$. This impulse has an amplitude $\bar{F}_{\text{imp}} > F_s$. The modulation of the width of the impulse results from the comparison of the displacement of the actual positioning system and that of a reference model. This method is widely used when simplicity and micrometric range positioning accuracy are required [**26, 27**]. As it will shown in the treatise below, this approach, developed to compensate macro-dynamic phenomena, could be applicable also to the pre-sliding region.

The approach is based on the physical model of Fig. 4 where only macro-dynamic phenomena are considered. In that case the dependence between the pulse width t_{imp} and the resulting displacement X is quadratic. In fact, the dynamic equilibrium equations of the considered translational model are

$$\begin{aligned} F_{\text{imp}} &= M\ddot{X} + c\dot{X} + F_{\text{c}} && \text{for } \dot{X} \neq 0 \\ M\ddot{X} &= 0 && \text{for } \dot{X} = 0, |F_{\text{imp}}| \leqslant F_{\text{s}} \\ F_{\text{imp}} &= M\ddot{X} + \text{sgn}(F_{\text{imp}})F_{\text{s}} && \text{for } \dot{X} = 0, |F_{\text{imp}}| > F_{\text{s}} \end{aligned} \tag{1}$$

In reference [**18**] it is shown that, integrating twice these equations and neglecting damping, the total displacement of the system can be expressed as

$$X = \frac{\bar{F}_{\text{imp}}(\bar{F}_{\text{imp}} - F_{\text{c}})}{2MF_{\text{c}}} t_{\text{imp}}^2 = b t_{\text{imp}}^2 \text{sgn}(\bar{F}_{\text{imp}}) \tag{2}$$

When viscous friction is present as well, the relation between pulse width and the resulting displacement is more complex

$$X = \frac{\bar{F}_{\text{imp}} t_{\text{imp}}}{c} - \frac{MF_{\text{c}}}{c^2} \ln\left[\frac{\bar{F}_{\text{imp}}}{F_{\text{c}}}\left(\text{e}^{t_{\text{imp}}c/M} - 1\right) + 1\right] \tag{3}$$

For short pulse widths equation (3) can be shown to be excellently approximated by equation (2), since for small velocities the force due to damping is negligible. Because of the variability of frictional effects, however, the coefficient of proportionality b between the square of the pulse width and the respective displacement in equation (2) has a significant stochastic component and can be determined only adaptively by using the classical Model Reference Adaptive Control (MRAC) or Self Tuning Regulator (STR) algorithms [**28**]. Figure 8 shows the block diagram of the MRAC system implemented as suggested by Yang and Tomizuka [**18**]. For this purpose the regulator is based on the characteristic quadratic equation (2), where the coefficient of proportionality b between the square of the pulse width t_{imp} and the resulting displacement X is determined by a Parameter Adaptation Algorithm (PAA). The input signals to this algorithm are pulse width, the actual displacement, and displacement X' that is

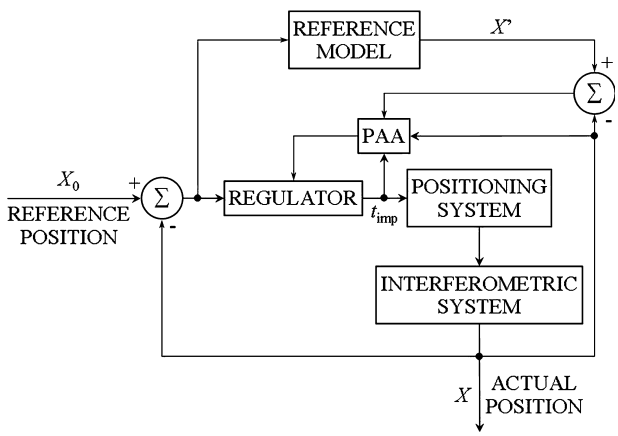

Fig. 8 MRAC algorithm

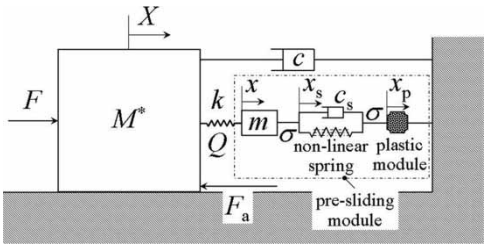

Fig. 9 Integrated system model

obtained using a linear reference model in which an ideal response of the system is assumed.

3.2 Compensation of macro- and micro-dynamics non-linearities

In the case of nanometric positioning, macro-dynamic non-linearities of the model of Fig. 4 have to be coupled with the pre-sliding model of Fig. 5. The resulting system is shown in Fig. 9 where the part of the overall system mass that is in the macro-dynamics regime is indicated with M^* while the remaining part, which is in pre-sliding, is designated with m. As already pointed out, when the system used in this work is in the micrometric regime, mass m corresponds practically to that of the linear slide. Stiffness k of the coupling of the two masses is large enough so that the difference between x and X can be considered negligible.

A mathematical model of the whole system is made. In principle the coupling of equation (1) with the reaction force Q due to pre-sliding, evaluated according to the model given in reference [**16**], is performed. The equilibrium equations of mass M become therefore

$$\begin{aligned} &F_{\text{imp}} = M^*\ddot{X} + c\dot{X} + F_{\text{c}} + Q && \text{for } \dot{X} \neq 0 \\ &M^*\ddot{X} + Q = 0 && \text{for } \dot{X} = 0, \left|F_{\text{imp}}\right| \leqslant F_{\text{s}} \\ &F_{\text{imp}} = M^*\ddot{X} + \text{sgn}(F_{\text{imp}})F_{\text{s}} + Q && \text{for } \dot{X} = 0, |F_{\text{imp}}| > F_{\text{s}} \end{aligned} \tag{4}$$

where $Q = k\ (X - x)$ is the force due to the micro-dynamics reactions on mass m, i.e. the part of the total mass of the system which is in pre-sliding regime.

The direct integration of these equations cannot, however, be done since the micro-dynamics model requires as input the time history of force Q. It is thus necessary to make use of an iterative procedure. Equations (4) have to be integrated in time considering the time history of displacement x and the resulting $Q(t)$ obtained in the previous iteration. The integration is performed up to the point when the system comes to rest. It is therefore possible to evaluate a new $X(t)$ and consequently a new time history of force Q, which is input into the pre-sliding module. Convergence is generally reached in few steps, i.e. when the new value of X in two consecutive iterations differs negligibly. The respective algorithm, encompassing macro-dynamic phenomena and the pre-sliding module of reference [**16**], has been implemented in MATLAB®.

It must be pointed out that, in the case when the dynamics conditions are such that the whole system is in the macro-dynamics regime, mass m vanishes and consequently, as $M^* = M$ and Q has to be set equal to zero, the set of equations (4) coincides with that given by equations (1).

3.3 Response of the system to impulsive loads of variable widths

Trying to extend the applicability of the control method developed by Yang and Tomizuka [**18**] to the case of nano-positioning, it becomes necessary to identify the dependence displacement versus pulse widths. Basically, it is necessary to establish whether the solution of equations (4) has still the quadratic form of equation (2), which was obtained solving the system of equations (1).

A numerical simulation according to the previously described procedure has thus been performed with impulses of constant amplitude $\bar{F}_{\text{imp}} = 1.25\ F_{\text{s}}$ and with gradually increasing widths up to 1000 ms. An experimental verification has also been performed by actuating through the DSP board the electro-mechanical system under consideration and measuring via the interferometric system the resulting displacements.

The obtained numerical and experimental results are shown in Fig. 10. The intervals of uncertainty of the measurements were obtained via repetitive ($n_{\text{s}} > 15$) tests. The mentioned position and time variability of friction implies, in fact, the necessity to employ a statistical approach. The results of the simulation are in perfect agreement with those given by equation (3) and thus, for larger impulse widths, rather different from those obtained with the quadratic relation of equation (2). These results are perfectly concordant with the average of the experimental results, whose dispersion is at the level of a few percent. It is important, however, that the simulation results, the

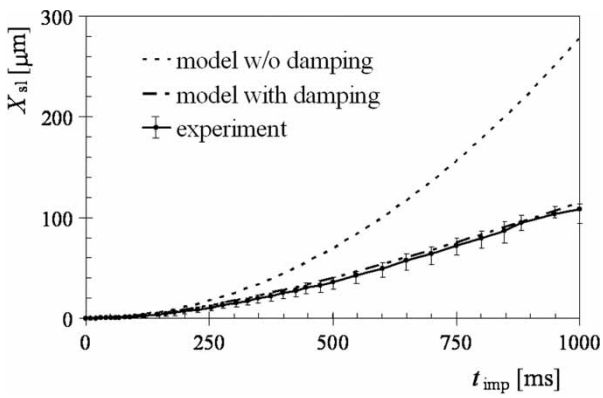

Fig. 10 Displacement vs. pulse width

analytical results of equations (2) and (3), as well as the experimental results are all approximated very well by the quadratic relation of equation (2) for pulse widths $t_{imp} \leqslant 200$ ms. This corresponds to displacements of the order of 10 μm. As clear from equation (2), larger values of the amplitude $\bar{F}_{\text{imp}}$ of the impulsive force would allow achieving larger values of displacements for equal pulse widths.

4 PROPOSED NANO-POSITIONING APPROACH

Comparing the data of Fig. 10 with those of Fig. 7, it is confirmed that, if the range of variation of pulse widths is limited to values where the quadratic characteristic is valid, the linear slide is in the pre-sliding displacement range. This means that, even if the amplitudes of the actuating forces are larger than those needed to overcome stiction, the duration of actuation is not long enough to induce breakaway and consequently to produce sliding. Yang and Tomizuka's model, developed to compensate macro-dynamic non-linearities, is therefore still valid when micro-dynamic phenomena are present as well. However, in this case the model parameters have a different physical meaning, since the frictional force F_a of the model shown in Fig. 9 does not account for the contribution of the slide, but only for that of the upstream elements, which is usually the prevailing one. However, due to the effect of speed ratios, generally the effective contribution of the micro-dynamic forces can be considered as a virtual variation of F_a and therefore is already taken into account by the MRAC algorithm used to adapt the value of the proportionality parameter b of equation (2). This implies also that usually the cumbersome trial-and-error phase in the determination of the parameters of the pre-sliding module can be avoided, since the adaptive nature of the algorithm takes into account the influence of the pre-sliding phenomena as well.

In conclusion, the suggested adaptive approach seems thus suited to compensate both the macro- and the micro-dynamics phenomena. Differently from the cited approaches used to achieve nano-positioning [**4**, **8**, **12**, **17**], the method proposed in this work does not hence require a dual control structure to be implemented.

However, in cases when the reference position is very large, the positioning speed can be improved using any traditional actuation scheme. In this work, this objective is achieved by using a simple PID control typology in which the proportional term is kept constant while the I and D terms are set to zero (P control); in other experimental configurations it might be necessary to use a real PD or PID control [**3**].

Based on the above considerations, a control procedure was implemented and its baseline structure is

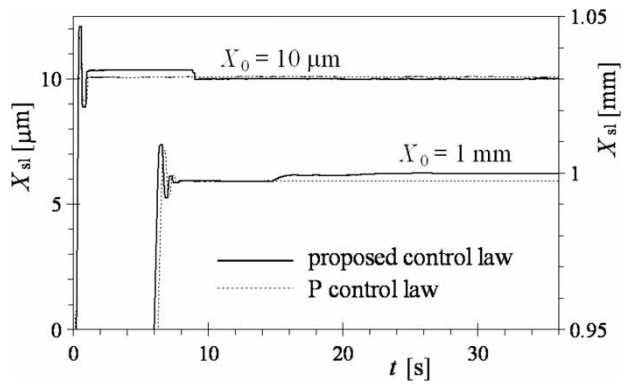

Fig. 11 Measured displacements for a 10 μm and for a 1 mm reference position

(a) the reference position X_0 is compared to the actual slide displacement X_{sl} measured via the interferometric system;
(b) if the obtained difference is very large, the system is actuated using P control up to the point when it comes to a rest;
(c) at this point actuation is performed by applying impulses of variable widths, where the width of the first impulse is determined by using a predefined (supposed) value of the coefficient of proportionality between the displacement and the square of the pulse width;
(d) the subsequent values of this coefficient are determined by an adaptive approach using the MRAC-type algorithm of Fig. 8.

Figure 11 shows the experimental results obtained by applying the described procedure in the case of a rather small reference position (10 μm) and a rather large one (1 mm). For comparison purposes, in the same figure are given also the results obtained by using the simple proportional control. In the case of the control scheme proposed in this work, the system is initially actuated following a P control law, which results in a high slope and a marked overshoot. The adaptive pulse width control is then applied resulting in a considerably smaller velocity bringing the system to the reference position with nanometric accuracy. In fact, several measurements performed with various reference positions by using the proposed approach, allowed establishing that in all the considered cases the positioning error was equal to the interval of uncertainty of the measurements of the laser interferometer system (i.e. the error was within ±20 nm), indicating that at least in some cases reached accuracy may even be better.

5 CONCLUSIONS

Several methods have been proposed in literature to achieve nanometric positioning. Generally these

approaches require off-line system identification and dual-mode control laws where the models used to describe, respectively, the macro- and the micro-dynamic friction regimes are usually different and quite complex.

In this work a simple and unique control typology has been proposed. The procedure is based on the adaptation of the width of the actuating impulsive force and it does not require a trial-and-error determination of the characteristic parameters of the complex micro-dynamics model. In fact, the pre-sliding effect is shown to be equivalent to a small perturbation of the macro-dynamics phenomenon so that the adaptive nature of the compensation of the latter counterbalances the consequences of the micro-dynamic effects as well. The adoption of the proposed pulse width approach to nano-positioning on short and longer travels confirms the validity of the physical interpretation of the observed phenomena. In fact, experiments show that in all the considered cases positioning within ±20 nm from the reference position has been obtained; this value corresponds to the precision of the laser interferometer.

ACKNOWLEDGEMENTS

The work was performed with the support of the 'Ultra-high precision compliant devices for micro and nanotechnology applications' project of the Croatian Ministry of Science, Education and Sports, the 'Theoretical and Experimental Analysis of Compliant Mechanisms for Micro- and Nanomechanical Applications' project of the Italian Ministry of University and Research, and the 'A Stronger Europe with MIcro- and NAnotechnologies (SEMINA)' project of the Swiss National Science Foundation.

REFERENCES

1 **Blau, P. J.** *Friction science and technology*, 1996 (CRC Press, UK).
2 **Slocum, A. H.** *Precision machine design*, 1992 (Prentice-Hall, USA).
3 **Armstrong-Helouvry, B., Dupont, P.,** and **Canudas de Wit, C.** A survey of models, analysis tools and compensation methods for the control of machines with friction. *Automatica*, 1994, **30**, 1083–1138.
4 **Chen, C. L., Jang, M. J.,** and **Lin, K. C.** Modeling and high-precision control of a ball-screw-driven stage. *Precis. Eng.*, 2004, **28**, 483–495.
5 **Courtney-Pratt, J. S.** and **Eisner, E.** The effect of a tangential force on the contact of metallic bodies. *Proc. R. Soc.*, 1957, **A 238**, 529–550.
6 **Futami, S., Furutani, A.,** and **Yoshida, S.** Nanometer positioning and its micro dynamics. *Nanotechnology*, 1990, **1**(1), 31–37.
7 **Ro, P. I.** and **Hubbel, P. I.** Model reference adaptive control of dual-mode micro/macro dynamics of ball screws for nanometer motion. *ASME J. Dyn. Sys., Meas. Control*, 1993, **115**, 103–108.
8 **Yau, H.-T.** and **Yan, J.-J.** Adaptive sliding mode control of a high-precision ball-screw-driven stage. *Nonlinear Anal.: Real World Appl.*, 2009, **10**(3), 1480–1489.
9 **Ro, P. I., Shim, W.,** and **Jeong, S.** Robust friction compensation for submicrometer positioning and tracking for a ball-screw-driven slide system. *Precis. Eng.*, 2000, **24**(2), 160–173.
10 **Sato, K., Nakamoto, K.,** and **Shimokohbe, A.** Practical control of precision positioning mechanism with friction. *Precis. Eng.*, 2004, **28**, 426–434.
11 **Siebenhaar, Ch.** Precise adjustment method using stroke impulse and friction. *Precis. Eng.*, 2004, **28**, 194–203.
12 **Tseng, Y.-T.** and **Liu, J.-H.** High-speed and precise positioning of an X–Y table. *Control Eng. Pract.*, 2002, **11**, 357–365.
13 **Canudas de Wit, C., Olsson, H., Astrom, K. J.,** and **Lischinsky, P.** A new model for control of systems with friction. *IEEE Trans. Autom. Control*, 1995, **40**(3), 419–425.
14 **Chen, C. L., Lin, K. C.,** and **Hsieh, C.** Presliding friction mode: modelling and experimental study with a ball-screw-driven set-up. *Math. Comp. Model. Dyn. Syst.*, 2005, **11**(4), 397–410.
15 **Worden, K., Wong, C. X., Parlitz, U., Hornstein, A., Engster, D., Tjahjowidodo, T., Al-Bender, F., Rizos, D. D.,** and **Fassois, S. D.** Identification of pre-sliding and sliding friction dynamics: grey box and black-box models. *Mech. Syst. Sign. Process.*, 2007, **21**, 514–534.
16 **Hsieh, C.** and **Pan, Y.-C.** Dynamic behavior and modelling of pre-sliding static friction. *Wear*, 2000, **242**, 1–17.
17 **Perng, M. H.** and **Wu, S. H.** A fast control law for nano-positioning. *Int. J. Mach. Tools Manuf.*, 2006, **46**, 1753–1763.
18 **Yang, S.** and **Tomizuka, M.** Adaptive pulse width control for precise positioning under the influence of stiction and Coulomb friction. *ASME J. Dyn. Sys., Meas. Control*, 1988, **110**, 221–227.
19 **Steinmetz, C. R.** Sub-micron position measurement and control on precision machine tools with laser interferometry. *Precis. Eng.*, 1990, **12**, 12–24.
20 **Lee, H. S.** and **Tomizuka, M.** Robust motion controller design for high-accuracy positioning systems. *IEEE Trans. Ind. Elec.*, 1996, **43**(1), 48–55.
21 **Armstrong-Helouvry, B.** Stick slip and control in low-speed motion. *IEEE Trans. Autom. Contr.*, 1993, **38**, 1483–1496.
22 **Canudas, C., Astrom, K. J.,** and **Braun, K.** Adaptive friction compensation in DC motor drives. In Proceedings of the IEEE International Conference on *Robotics & automation*, San Francisco, 1986, pp. 1556–1561.
23 **Dupont, P. E.** Avoiding stick-slip through PD control. *IEEE Trans. Autom. Contr.*, 1994, **39**, 1094–1097.
24 **Smith, M. H., Annwamy, A. M.,** and **Slocum, A.** Adaptive control strategies for a precision machine tool axis. *Precis. Eng.*, 1995, **17**, 12–24.
25 **Lin, T.-Z., Pan, Y.-C.,** and **Hsieh, C.** Precision-limit positioning of direct drive systems with the existence of friction. *Control. Eng. Pract.*, 2003, **11**, 233–244.
26 **Rathbun, D. B., Berg, M. C.,** and **Buffinton, K. W.** Pulse width control for precise positioning of structurally

flexible systems subject to stiction and Coulomb friction. *ASME J. Dyn. Sys., Meas. Control*, 2004, **126**, 131–138.

27 **van de Wijdeven, J. J. M.** and **Singh, T.** Adaptive pulse amplitude pulse width control of systems subject to Coulomb and viscous friction. In Proceedings of the American Control Conference, Denver, 2003, pp. 1068–1073.

28 **Astrom, K. J.** Theory and applications of adaptive control – a survey. *Automatica*, 1983, **19**, 471–486.

APPENDIX

Notation

b	coefficient of proportionality for pulse width control
c	viscous damping coefficient
c_s	viscous damping coefficient of pre-sliding module
F	applied force
F_a	friction force
F_c	Coulomb friction
F_{imp}	pulse force of finite width t_{imp}
$\bar{F}_{imp}$	amplitude of F_{imp}
F_s	static friction
k	stiffness of coupling between mass M^* and mass m
k_1, k_2, β	non-linear spring parameters of pre-sliding model
m	pre-sliding translational mass
M	equivalent translational mass of the system
M_f	frictional torque
M^*	macro-dynamics translational mass
n_s	sample size
Q	input force to pre-sliding module
t	time
t_{imp}	pulse width
x	displacement of mass m
x_s, x_p	non-linear spring and plastic displacement of mass m
X	displacement of the mass in the macro-dynamics regime
X_{sl}	slide displacement
X_0	reference position
X'	displacement as calculated in MRAC reference model
α, λ, n	parameters of plastic module in pre-sliding model
σ	pre-sliding friction force
ω	angular velocity